

# Electromagnetic form factors of hyperons in the timelike region: A short review

Ling-Yun Dai<sup>1,2,\*</sup>, Johann Haidenbauer<sup>3,†</sup> and Ulf-G. Meißner<sup>4,3,5,6‡</sup>

<sup>1</sup>*School for theoretical Physics, School of Physics and Electronics, Hunan University, Changsha 410082, China*

<sup>2</sup>*Hunan Provincial Key Laboratory of High-Energy Scale Physics and Applications, Hunan University, Changsha 410082, China*

<sup>3</sup>*Institute for Advanced Simulation (IAS-4), Forschungszentrum Jülich GmbH, D-52425 Jülich, Germany*

<sup>4</sup>*Helmholtz Institut für Strahlen- und Kernphysik and Bethe Center  
for Theoretical Physics, Universität Bonn, D-53115 Bonn, Germany*

<sup>5</sup>*Peng Huanwu Collaborative Center for Research and Education, Beihang University, Beijing 100191, China and*

<sup>6</sup>*Tbilisi State University, Tbilisi 0186, Georgia*

We review recent experimental and theoretical results for the electromagnetic form factors of hyperons ( $Y$ ) in the timelike region, accessible in the reactions  $e^+e^- \rightarrow \bar{Y}Y$ . Specifically, we focus on the final states  $\bar{\Lambda}\Lambda$ ,  $\bar{\Lambda}\Sigma^0/\bar{\Sigma}^0\Lambda$ ,  $\bar{\Sigma}\Sigma$ ,  $\bar{\Xi}\Xi$ , and  $\bar{\Omega}\Omega$ . The  $\bar{\Lambda}_c\Lambda_c$  system is also discussed.

*Introduction.*— Electromagnetic form factors (EMFFs) constitute an important tool for elucidating the internal structure of baryons. Indeed, the EMFFs of the proton (and with some restrictions of the neutron) in the space-like region have been mapped out quite successfully by performing electron-proton ( $ep$ ) scattering experiments and those measurements have provided clear evidence for the non-elementary nature of the nucleons. For recent reviews see [1–5].

For the hyperons ( $Y$ ), that is the  $\Lambda$ ,  $\Sigma$ , or  $\Xi$ , the situation is very different. Due to their short lifetime, preparing a hyperon target is virtually impossible, and thus, electron scattering experiments that allow access to the EMFFs in the spacelike region are not available. However, an experimental determination of the form factors is possible in the timelike region, namely via the reaction  $e^+e^- \rightarrow \bar{Y}Y$ . Some pioneering measurements have already been performed around two decades ago or even before [6, 7]. However, only recently has there been an enormous increase in the wealth of data available for hyperons. Not only an impressive variety of hyperons have been measured, from the  $\Lambda$  up to the  $\Omega$ , but also a wide range of energies has been covered, reaching (in most cases) from close to the threshold at twice the hyperon mass up to several GeV.

In this review, we focus the development over the past few years, on the experimental as well as on the theoretical side. The EMFFs in the timelike region are connected with those in the spacelike region by dispersion relations, which follow from unitarity and analyticity [1, 4]. However, at the same time, they reflect different physical aspects of the baryons. As already mentioned above, in the spacelike region, they provide information on the electromagnetic structure of the baryons. In the timelike region, other features can be studied. For example, close to the reaction threshold the interaction of the produced  $\bar{Y}Y$  pair should have a noticeable influence on the energy dependence of the cross section and, in turn, on the EMFFs. Furthermore, the coupling of the photon to vector mesons, exploited in the vector-meson dominance (VMD) model, could be prominently seen in the cross section, provided that there is also a non-zero coupling

to the  $\bar{Y}Y$  state. At very high energies, one expects the onset of perturbative QCD (pQCD), as reflected in the energy dependence that follows from the quark-counting rules. Besides, Ref. [8] suggests that the timelike EMFFs of the nucleons reflect the distributions of polarized electric charges induced by hard photons. This conjecture can be extended to the hyperons if it is confirmed.

The review is structured in the following way: In the next section, we provide the essentials of the formalism. After that, we summarize the experimental situation and give a brief glimpse into the theoretical approaches. Subsequently, a more detailed discussion of the cross sections and EMFFs for the  $\Lambda$ ,  $\Sigma^+$ ,  $\Sigma^0$ ,  $\Sigma^-$ ,  $\Omega$ , and  $\Lambda_c$ , and of the  $\Lambda\Sigma^0$  transition form factor is given, where the emphasis is on energies not too far from the thresholds. The review closes with a brief summary.

*Formalism and observables.*— Under the assumption that the reaction  $e^+e^- \rightarrow \bar{Y}Y$  proceeds via one-photon exchange, the differential cross section and the EMFFs  $G_E^Y$  and  $G_M^Y$  are related by

$$\frac{d\sigma}{d\Omega} = \frac{\alpha^2\beta}{4s} C(s) \left[ |G_M^Y(s)|^2 (1 + \cos^2\theta) + \frac{4M_Y^2}{s} |G_E^Y(s)|^2 \sin^2\theta \right], \quad (1)$$

where  $Y$  generically denotes the baryons  $\Lambda$ ,  $\Sigma$ ,  $\Xi$ ,  $\Omega$ , and  $\Lambda_c$ , and  $\bar{Y}$  stands for the corresponding anti-particles. Here,  $\alpha = 1/137.036$  is the electromagnetic fine-structure constant and  $\beta = k_Y/k_e$  a phase-space factor, where  $k_Y$  and  $k_e$  are the center-of-mass three-momenta in the  $\bar{Y}Y$  and  $e^+e^-$  systems, respectively, related to the total energy via  $\sqrt{s} = 2\sqrt{M_Y^2 + k_p^2} = 2\sqrt{m_e^2 + k_e^2}$ . Further,  $m_e$  ( $M_Y$ ) is the electron (hyperon) mass. For charged baryons, the Coulomb effect is present which is taken into account via the  $S$ -wave Sommerfeld-Gamow factor  $C(s)$ , given by  $C = y/(1 - e^{-y})$  with  $y = \pi\alpha M_Y/k_Y$ . In general, we omit the superscript  $Y$  from the  $G$ 's in the following because it is anyway clear from the context in which hyperon is discussed. As noted, the cross section as written in Eq. (1) results from the one-photon exchange

approximation and by setting the electron mass  $m_e$  to zero (then  $\beta = 2k_Y/\sqrt{s}$ ). In this case, the total angular momentum is fixed to  $J = 1$  and the  $e^+e^-$  and  $\bar{Y}Y$  systems can be only in the partial waves  $^3S_1$  and  $^3D_1$ . Note further that the EMFFs in the timelike region are complex quantities.

The integrated reaction cross section is readily found to be

$$\sigma_{e^+e^- \rightarrow \bar{Y}Y} = \frac{4\pi\alpha^2\beta}{3s} C(s) \left[ |G_M(s)|^2 + \frac{2M_Y^2}{s} |G_E(s)|^2 \right]. \quad (2)$$

As is clear from Eqs. (1) and (2) a separation of  $G_E$  and  $G_M$  is only possible from the differential cross section. Since just a few measurements of that observable have been performed so far, another quantity is often considered, namely the effective baryon form factor  $G_{\text{eff}}$  which is defined by

$$|G_{\text{eff}}(s)| = \sqrt{\frac{\sigma_{e^+e^- \rightarrow \bar{Y}Y}(s)}{\frac{4\pi\alpha^2\beta}{3s} C(s) \left[ 1 + \frac{2M_Y^2}{s} \right]}}. \quad (3)$$

This quantity provides a measure for the deviation of the experimental cross section from the point-like one.

Finally, the relative phase of  $G_E$  and  $G_M$ , defined by the relation  $G_E/G_M = \exp(i\Delta\phi) |G_E/G_M|$ , can be only determined from spin-dependent observables, for example, it can be extracted from the analyzing power  $A_y$ , which is given by [9]

$$A_y = \frac{\frac{2M_Y}{\sqrt{s}} \sin 2\theta \text{Im} G_E^*(s) G_M(s)}{|G_M(s)|^2 (1 + \cos^2\theta) + \frac{4M_Y^2}{s} |G_E(s)|^2 \sin^2\theta}. \quad (4)$$

*Overview of experiments.*— Cross section data are available for  $e^+e^- \rightarrow \bar{\Lambda}\Lambda$  [6, 7, 10–13],  $e^+e^- \rightarrow \bar{\Lambda}\Sigma^0 + \text{c.c.}$  [6, 7, 14],  $e^+e^- \rightarrow \bar{\Sigma}\Sigma$  [7, 10, 15–20],  $e^+e^- \rightarrow \bar{\Xi}\Xi$  [10, 21–24],  $e^+e^- \rightarrow \bar{\Omega}\Omega$  [10, 25], and  $e^+e^- \rightarrow \bar{\Lambda}_c\Lambda_c$  [26–28]. For an overview of data from the BESIII Collaboration see also [29]. One essential advantage of hyperons is that the self-analyzing character of their weak decay allows one to determine also the polarization as well as spin-correlation parameters. With those observables one can determine the relative phase between  $G_E$  and  $G_M$  [9], as already mentioned. However, so far, detailed information like the aforementioned polarizations or differential cross sections is only available for a few  $\bar{B}B$  channels, namely  $\bar{\Lambda}\Lambda$  [7, 12],  $\bar{\Sigma}^-\Sigma^+$  [15, 17], and  $\bar{\Lambda}_c\Lambda_c$  [27, 28].

*Theoretical approaches.*— At low energies, the energy dependence of the  $e^+e^- \rightarrow \bar{Y}Y$  cross section should be strongly influenced by the final-state interactions (FSI) in the  $\bar{Y}Y$  system. This has been observed for protons [30] (and references therein) and it is likewise expected for hyperons. Therefore, such data constitute a testing

ground and source of information on the interaction between the produced  $\bar{Y}Y$  pair. The information is complementary to the one from  $\bar{p}p$  induced production of  $\bar{Y}Y$  systems studied with the LEAR facility at CERN [31]. FSI effects due to  $\bar{N}N$  and  $\bar{Y}Y$  interactions have been the focus of our studies [32–36] and those of others too, see, e.g. [37–44].

The formalism for the inclusion of the FSI in the  $\bar{Y}Y$  systems applied by us is described in detail in Refs. [30, 33]. Here, we restrict ourselves to an illustration; see Fig. 1.  $G_M^0$  and  $G_E^0$  represent the bare vertices or bare form factors, respectively, which we assume to be constants. Since  $G_M^0 = G_E^0$  at the reaction threshold due to kinematical constraints [30], there is, in general, only a single (complex) parameter that enters the calculation. In practice, it is a normalization factor to be fixed from the measured cross sections. The physical (dressed) EMFFs  $G_E$  and  $G_M$  acquire their energy (momentum) dependence in their evaluation in distorted wave Born approximation, based on a  $\bar{Y}Y \rightarrow \bar{Y}Y$  amplitude (half-off-shell  $T$ -matrix) which we take from our analyses of the reactions  $\bar{p}p \rightarrow \bar{\Lambda}\Lambda$ ,  $\bar{\Lambda}\Sigma^0 + \text{c.c.}$ ,  $\bar{\Sigma}\Sigma$ ,  $\bar{\Xi}\Xi$  that were measured in the PS170 experiment at the LEAR facility at CERN [31]. The intermediate states  $\bar{Y}'Y'$  are restricted to  $\bar{\Lambda}\Lambda$  ( $\bar{\Lambda}\Sigma^0/\bar{\Sigma}^0\Lambda$ ) in the reactions  $e^+e^- \rightarrow \bar{\Lambda}\Lambda$  ( $e^+e^- \rightarrow \bar{\Lambda}\Sigma^0 + \text{c.c.}$ ), and consist of  $\bar{\Sigma}^-\Sigma^+$ ,  $\bar{\Sigma}^0\Sigma^0$ ,  $\bar{\Sigma}^+\Sigma^-$  for the three  $e^+e^- \rightarrow \bar{\Sigma}\Sigma$  channels, and of  $\bar{\Xi}^0\Xi^0$  and  $\bar{\Xi}^+\Xi^-$  for the two  $e^+e^- \rightarrow \bar{\Xi}\Xi$  channels.

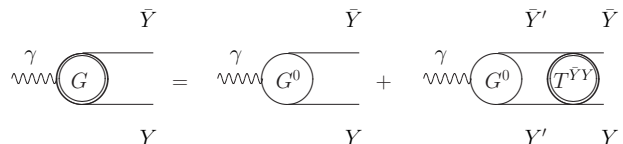


FIG. 1. Illustration of the treatment of the FSI in the reaction  $e^+e^- \rightarrow \bar{Y}Y$ . Here,  $G^0$  denotes the bare EMFFs and  $T^{\bar{Y}Y}$  is the  $\bar{Y}'Y' \rightarrow \bar{Y}Y$  reaction amplitude.

In the VMD model, the virtual photon couples to the baryons through vector mesons [2, 45, 46]. The standard vector mesons included in such studies are the  $\rho$ , the  $\omega$ , and also the  $\phi$ . However, their poles lie in the unphysical region and, in particular, well below the  $\bar{Y}Y$  thresholds, so that there is only a moderate effect on the energy dependence of the  $e^+e^- \rightarrow \bar{Y}Y$  cross section. This is different for the  $\phi(2170)$  whose pole is located fairly close to the  $\bar{\Lambda}\Lambda$  threshold. See Ref. [47] for a discussion in the  $\bar{p}p$  system. A prominent effect is also expected from the  $\psi(3770)$  resonance. In actual parameterizations of the  $e^+e^- \rightarrow \bar{Y}Y$  amplitudes within the VMD model, additional vector mesons are usually introduced. The imaginary part of the EMFFs is generated by including the finite width of the vector mesons. Finally, in general, a so-called intrinsic form factor of dipole form,  $g(s) = 1/(1 - \gamma s)^2$ , is multiplied where the parameter  $\gamma$  is adjusted to the data.

At sufficiently high energies one expects to see the onset of pQCD [48, 49], characterized by an energy dependence that follows from the so-called quark counting rules, see also the review [2]. A QCD-inspired model for the EMFFs of hyperons with focus on the perturbative regime of QCD has been proposed by Ramalho et al. [50–52]. It is an extension of their covariant spectator quark model in the spacelike regime to the timelike region [50]. In this context, we should also mention the simple pQCD-inspired parameterization by [53] and the one utilized in various papers by BESIII, taken from [2], which reproduce the energy dependence of the  $\bar{Y}Y$  EMFFs in the timelike region reasonably well, except for the threshold region.

Discussions of the hyperon form factors in the timelike region from other perspectives can be found in [54, 55].

For completeness, let us mention that spacelike EMFFs of hyperons are considered in [56, 57]. See also [58, 59].

$e^+e^- \rightarrow \bar{\Lambda}\Lambda$  and the EMFFs of the  $\Lambda$ .— Here, new cross section data have become available last year from BESIII [13]. The data in the near-threshold region are presented in Fig. 2, together with some theory results from the literature. The predictions from Refs. [33, 34] are based on FSI effects of  $\bar{\Lambda}\Lambda$  potentials established in studies of the reaction  $\bar{p}p \rightarrow \bar{\Lambda}\Lambda$  [60, 61]. In fact, the reaction  $\bar{p}p \rightarrow \bar{\Lambda}\Lambda$  has been extensively investigated in the PS185 experiment, and data are available for total and differential cross sections as well as for spin-dependent observables, down to energies very close to the reaction threshold, see e.g., the review in Ref. [31]. Thus, those  $\bar{\Lambda}\Lambda$  potentials are fairly well constrained by data.

The results are shown as bands that represent the model uncertainties. Obviously, the  $\bar{\Lambda}\Lambda$  FSI predicts a basically flat behavior of the cross section, quite in line with the energy dependence of the BaBar data [7]. On the other hand, the BESIII data point from 2018 at 2232.4 MeV [11] (filled square), i.e. just about 1 MeV above the  $\bar{\Lambda}\Lambda$  threshold ( $2M_\Lambda = 2231.37$  MeV), deviates from the overall trend and is not reproduced by the calculation. The already mentioned new BESIII data from 2023 [13] (open circles) are consistent with the other measurements in the threshold region within the uncertainties. In addition, they seem to support a tendency towards a more regular threshold behavior. Indeed, it has been shown that the data can be described by a conventional FSI [41], cf. the dotted line, though it remains unclear whether in that case the required  $\bar{\Lambda}\Lambda$  interaction is compatible with constraints from the  $\bar{p}p \rightarrow \bar{\Lambda}\Lambda$  data.

Data for  $|G_E/G_M|$  and  $\Delta\phi$  are available at a few energies [7, 12] and are discussed in [34].

Results for  $\bar{\Lambda}\Lambda$  within the VMD approach have been presented in Refs. [63, 65–67]. Besides the standard  $\omega$  and  $\phi$  contributions the  $\omega(1420)$ ,  $\omega(1650)$ ,  $\phi(1680)$ ,  $\phi(2170)$  have been included in [65]. In Ref. [67] various

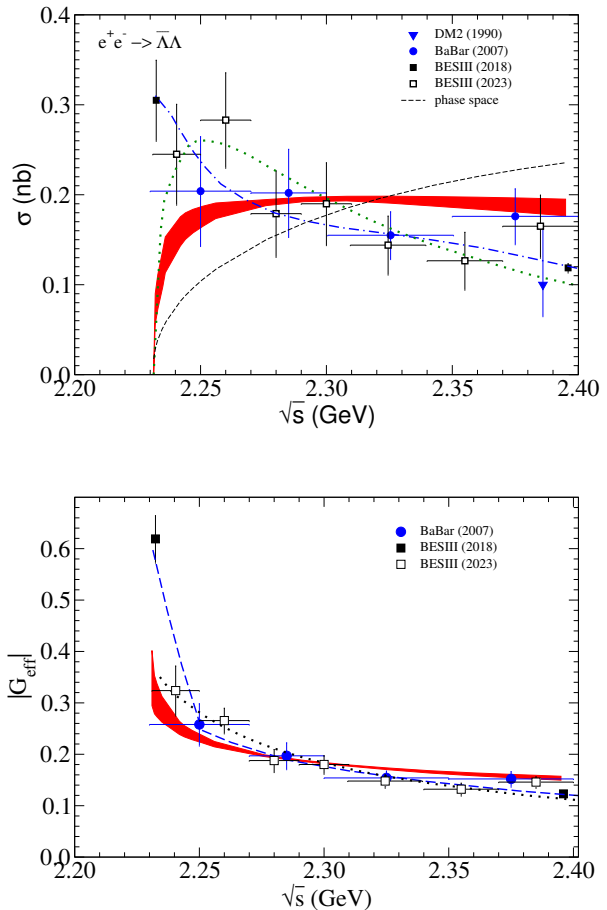


FIG. 2. Cross section for  $e^+e^- \rightarrow \bar{\Lambda}\Lambda$  and pertinent  $G_{\text{eff}}$ . Results from Refs. [33, 34] based on the  $\bar{\Lambda}\Lambda$  FSI fixed in [61] are shown by the red band, while the dotted line is the FSI fit from [41]. The dashed-dotted and dashed lines are VMD results from [62] and [63], respectively.

broad  $\phi(nS)$  and  $\phi(nD)$  states with masses between 2423 and 2924 MeV have been taken into account. A similar plethora of states has also been considered in [66]. The work of Li et al. [63] explores specifically the unusual behavior at the  $\bar{\Lambda}\Lambda$  threshold. It demonstrates that the description of the BESIII close-to-threshold data point requires to add a narrow and so far unknown resonance whose mass coincides with the  $\bar{\Lambda}\Lambda$  threshold within its width ( $M_x = 2230.9$  MeV,  $\Gamma_x = 4.7$  MeV). The behavior at the threshold has also been studied by Cao et al. [62]. In this case, a background motivated by pQCD is adapted, supplemented with a suitably adjusted contribution of the sub-threshold resonance  $\phi(2170)$  in combination with an additional resonance at 2340 MeV. The results of the latter calculations are reproduced in Fig. 2 for illustration, cf. the dash-dotted line.

An exemplary result of what can be achieved within the VMD approach over a larger energy region is shown in Fig. 3. This calculation is taken from Ref. [64] where

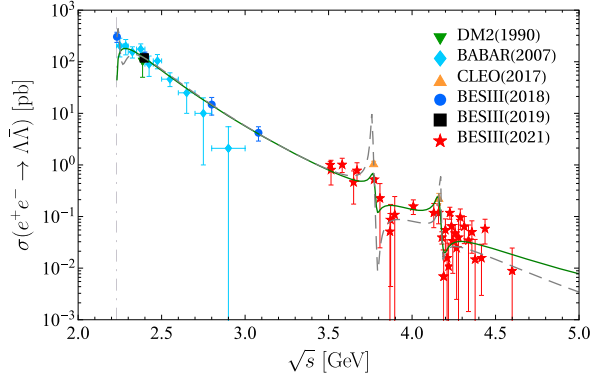


FIG. 3. Cross section for  $e^+e^- \rightarrow \bar{\Lambda}\Lambda$ . Results of a dispersion-theoretical analysis by Lin et al. taken from [64].

a dispersion-theoretical analysis of the  $\Lambda$  EMFFs in the timelike region has been performed. Here, several narrow and also broad vector mesons (poles) in the mass region of 1965 MeV to 4170 MeV are included when fitting to the  $e^+e^- \rightarrow \bar{\Lambda}\Lambda$  data, among others, the  $\phi(2170)$  and the  $\psi(3770)$ . One can see that the cross section can be rather well described up to  $\sqrt{s} \approx 5$  GeV. Further studies of  $e^+e^- \rightarrow \bar{\Lambda}\Lambda$  can be found in [39, 65, 68].

$e^+e^- \rightarrow \bar{\Lambda}\Sigma^0 + c.c.$  and the transition EMFFs for  $\Lambda\Sigma^0$ . – For the reaction  $e^+e^- \rightarrow \bar{\Lambda}\Sigma^0 + c.c.$ , so far, only cross sections are available. Pertinent results are presented in Fig. 4. Recently, BESIII has provided new data [14] (squares). Previously, only two measurements had been available [6, 7] where the one from DM2 [6] is actually an upper limit.

Before we start discussing the FSI effects, let us emphasize that, compared to  $\bar{p}p \rightarrow \bar{\Lambda}\Lambda$ , the experimental situation for the reaction  $\bar{p}p \rightarrow \bar{\Lambda}\Sigma^0 + c.c.$  is much less satisfactory, and for  $\bar{p}p \rightarrow \bar{\Sigma}\Sigma$  basically only a single measurement exists [31]. In case of  $\bar{p}p \rightarrow \bar{\Xi}\Xi$ , only upper bounds for the reaction cross section are available. Thus, the quality and quantity of constraints on the  $\bar{Y}Y$  interactions that have been applied in [34] to obtain the results for the  $e^+e^- \rightarrow \bar{Y}Y$  channels in question are much more limited. This should be kept in mind. Also, note that in Ref. [34] the normalization (i.e., the bare form factors  $G_E^0, G_M^0$ ) have been fixed to the BaBar data, so that the cross sections are 0.04 nb at 2.4 GeV.

Overall, the  $\bar{\Lambda}\Sigma^0 + c.c.$  cross section is noticeably smaller than that for  $\bar{\Lambda}\Lambda$ . However, like the latter, it remains practically constant over the energy region considered and does not follow the phase-space behavior, at least according to the BaBar measurement [7]. The predictions based on the  $\bar{Y}Y$  models established in Ref. [61] agree nicely with that behavior. The new data from BESIII [14] suggest a near-threshold cross section that is almost twice as large and possibly more energy-dependent, too.

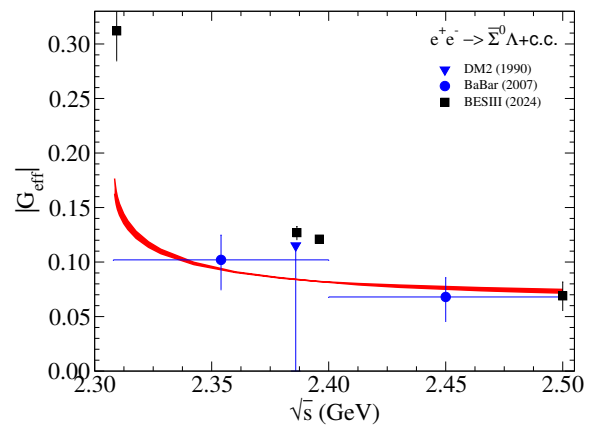
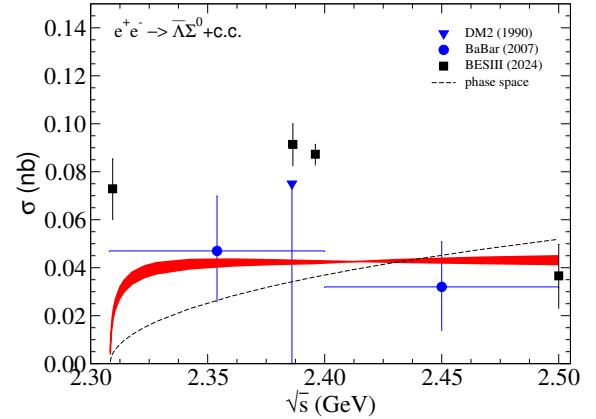


FIG. 4. Cross section for  $e^+e^- \rightarrow \bar{\Lambda}\Sigma^0 + c.c.$  and pertinent  $G_{\text{eff}}$ . Data are from DM2 [6], BaBar [7], and BESIII [14]. The theory result (band) is from [34].

$e^+e^- \rightarrow \bar{\Sigma}\Sigma$  and the EMFFs of the  $\Sigma$ . – Here, new measurements have been reported by the Belle Collaboration [20] ( $\bar{\Sigma}^-\Sigma^+$  and  $\bar{\Sigma}^0\Sigma^0$  cross sections), and by BESIII ( $\bar{\Sigma}^-\Sigma^+$  cross sections [18] and values for  $|G_E/G_M|$  and  $\Delta\phi$  [17]). An overview of the situation near the threshold is provided in Figs. 5 and 6.

As already emphasized above, the rather limited information on the  $\bar{p}p \rightarrow \bar{\Sigma}\Sigma$  reaction [31] did not allow to constrain the  $\bar{\Sigma}\Sigma$  interaction in [61] reliably. Thus, the  $e^+e^- \rightarrow \bar{\Sigma}\Sigma$  results of [34], shown as bands in Fig. 5, have primarily an exploratory character. Nonetheless, it turned out that the energy dependence on the channels  $e^+e^- \rightarrow \bar{\Sigma}^-\Sigma^+, \bar{\Sigma}^+\Sigma^-$ , where data at low energies were available at the time when that study was performed, can be roughly described. Moreover, it was found that the  $\bar{\Sigma}\Sigma$  FSI introduces a strong interplay between the  $e^+e^- \rightarrow \bar{\Sigma}^-\Sigma^+, \bar{\Sigma}^0\Sigma^0, \bar{\Sigma}^+\Sigma^-$  results in the near-threshold region.

The new data for  $\bar{\Sigma}^-\Sigma^+$  [18, 20] suggest a cross section significantly larger than what had been reported before while those for  $\bar{\Sigma}^0\Sigma^0$  [16, 20] indicate that the energy

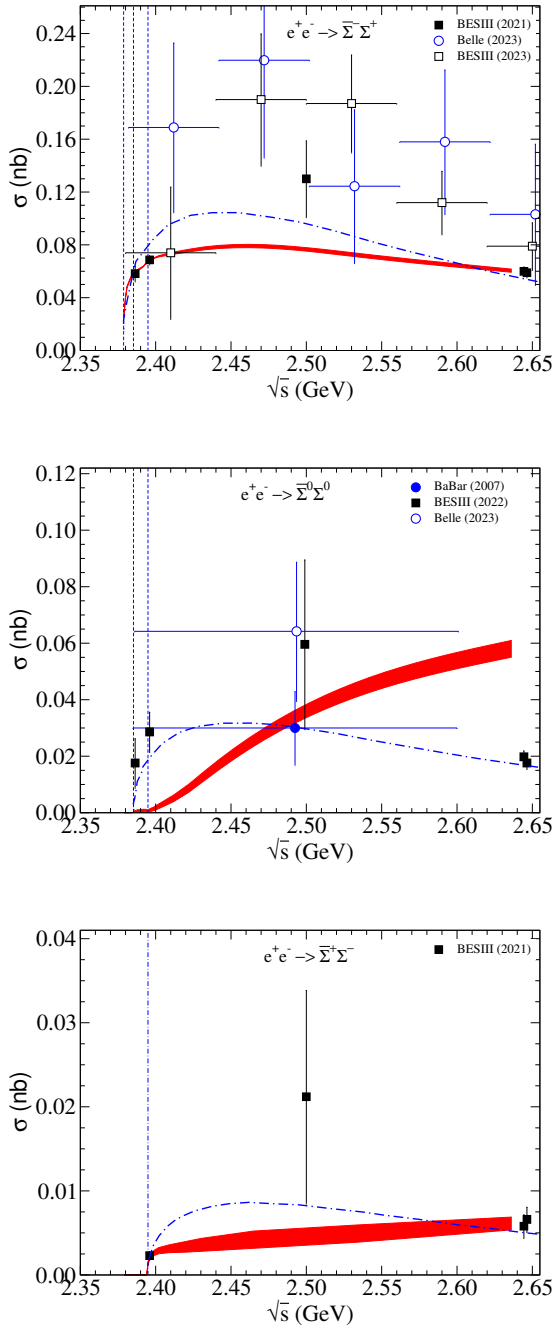


FIG. 5. Cross sections for  $e^+e^- \rightarrow \bar{\Sigma}^-\Sigma^+$ ,  $\bar{\Sigma}^0\Sigma^0$ ,  $\bar{\Sigma}^+\Sigma^-$  (top left, right, bottom). Data are from BaBar [7], BESIII (2020) [15], (2021) [16], and (2023) [18], and Belle [20]. Predictions from [34] based on FSI effects are shown by bands. The dash-dotted line is the VMD result from [69]. Vertical lines indicate the  $\bar{\Sigma}\Sigma$  thresholds.

dependence here could be similar to that in the other  $\bar{\Sigma}\Sigma$  channels. Indeed, to some extent, the experimental situation for  $\bar{\Sigma}^-\Sigma^+$  has become confusing when one compares the earlier high-precision measurements by BESIII [15] (filled squares) very close to the threshold with the overall trend of the other data. Hopefully, future exper-

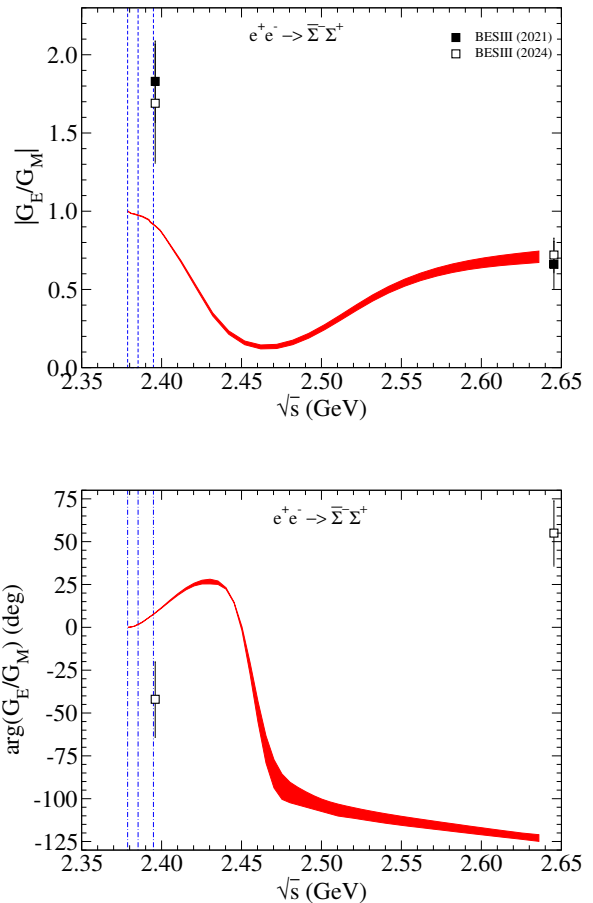


FIG. 6. Form factor ratio  $|G_E/G_M|$  and phase  $\Delta\phi$  for  $e^+e^- \rightarrow \bar{\Sigma}^-\Sigma^+$ . Data are from [15, 17]. The theory results are from [34]. Vertical lines indicate the  $\bar{\Sigma}\Sigma$  thresholds.

iments will allow one to establish reliably the energy dependence of the  $\bar{\Sigma}^-\Sigma^+$  cross section at low energies, but also the ones of the other  $\bar{\Sigma}\Sigma$  channels. The same applies to other observables like the ratio  $|G_E/G_M|$  or the relative phase between  $G_E$  and  $G_M$ . The latter, so far, measured only for  $\bar{\Sigma}^-\Sigma^+$  [17], seem to be very sensitive to the details of the  $\bar{\Sigma}\Sigma$  interaction as one can conclude from Fig. 6. But concrete conclusions on the  $\bar{\Sigma}\Sigma$  dynamics are difficult to draw from just two data points. In any case, since  $G_E = G_M$  at the threshold, large values for  $|G_E/G_M|$  and  $\Delta\phi$  so close to the threshold, as indicated by the BESIII experiment are difficult to achieve with a regular  $\bar{Y}Y$  interaction. Most likely, it would require again the introduction of a hypothetical resonance.

Calculations for the EMFFs of the  $\Sigma$  within the VMD approach can be found in two publications [69, 70], where in both works  $\rho$ ,  $\omega$ , and  $\phi$  are taken as the starting point. Results for all  $\Sigma$  channels have been reported in Ref. [69]. Those are included in Fig. 5; see the dash-dotted lines. As one can see, with that approach the energy dependence in all three channels can be reproduced fairly well.

Results for  $\Sigma^+$  and  $\Sigma^-$  can be found in Ref. [70], and those show a comparable agreement with the empirical information.

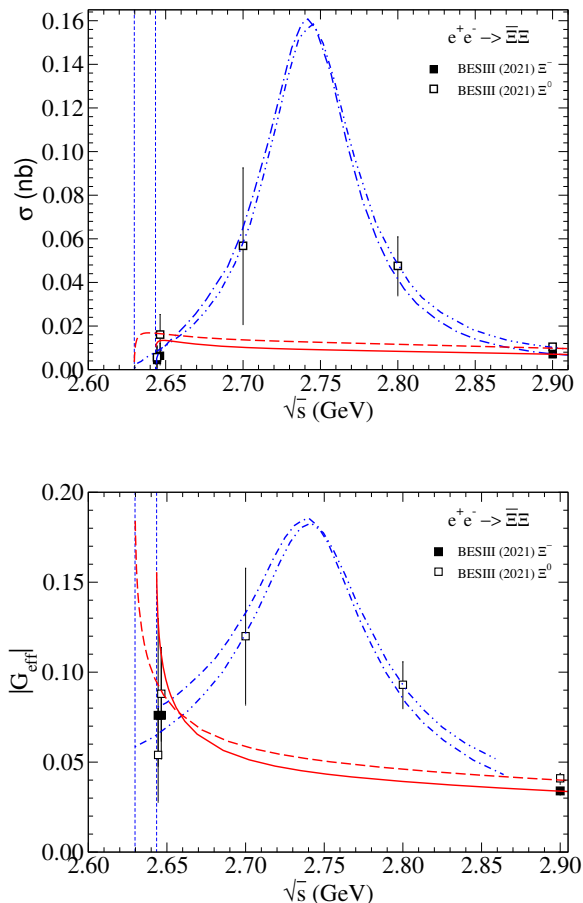


FIG. 7. Cross sections for  $e^+e^- \rightarrow \bar{\Xi}^0\Xi^0$  and  $e^+e^- \rightarrow \bar{\Xi}^+\Xi^-$ . The data are from [21] and [22]. Results based on  $\bar{\Xi}\Xi$  FSI effects [34] are shown by the solid and dashed lines. The dash-dotted (dash-double-dotted) line is the VMD result from [69]. Vertical lines indicate the  $\bar{\Xi}\Xi$  thresholds.

$e^+e^- \rightarrow \bar{\Xi}\Xi$  and the EMFFs of the  $\Xi$ .— Near-threshold measurements for  $e^+e^- \rightarrow \bar{\Xi}^+\Xi^-$  have been published by BESIII in 2020 [21] and soon afterwards also cross sections for  $\bar{\Xi}^0\Xi^0$  [22]. Ref. [34] included already some predictions for the reaction  $e^+e^- \rightarrow \bar{\Xi}\Xi$ , based on a  $\bar{\Xi}\Xi$  FSI [71] afflicted by similar shortcomings as those for  $\bar{\Lambda}\Sigma^0$  and  $\bar{\Sigma}\Sigma$ , see above. Since at the time when the calculation was performed only experimental information on  $e^+e^- \rightarrow \bar{\Xi}^+\Xi^-$  was available [21], the relative magnitude of the  $\bar{\Xi}^+\Xi^-$  and  $\bar{\Xi}^0\Xi^0$  channels could not be fixed, and only results in the isospin channels were shown. Now, results for both charge channels can be established, and those are presented in Fig. 7 together with the data for  $e^+e^- \rightarrow \bar{\Xi}^+\Xi^-, \bar{\Xi}^0\Xi^0$ . Thereby we assumed that the cross section for  $\bar{\Xi}^0\Xi^0$  is slightly larger than the one for

$\bar{\Xi}^+\Xi^-$ , as indicated by the data points at 2.9 GeV. It should be said that the empirical cross section ratio is practically compatible with unity when considered over a larger energy range [22].

An investigation of the reaction  $e^+e^- \rightarrow \bar{\Xi}\Xi$  in the VMD approach can be found in Ref. [69]. Here in addition to  $\rho$ ,  $\omega$ , and  $\phi$  two broad poles at 2.742 and 2.993 MeV have been added. Those results are reproduced in Fig. 7, cf. the dash-dotted and dash-double-dotted lines. Obviously, with those vector mesons one can reproduce all data points in the displayed energy region perfectly. Nonetheless, it would be good to perform further experiments in order to reliably confirm or disprove a resonance-like behavior.

$e^+e^- \rightarrow \bar{\Omega}\Omega$  and the EMFFs of the  $\Omega$ .— First measurements of the reaction  $e^+e^- \rightarrow \bar{\Omega}\Omega$  had been reported already 10 years ago by CLEO [10], while more extended measurements have been performed only recently [25]. However, the cross section turned out to be practically compatible with zero within the achieved accuracy. Moreover, there are no data close to the  $\bar{\Omega}\Omega$  threshold. A theoretical interpretation of the CLEO data has been attempted in [50, 51] within a pQCD inspired model.

$e^+e^- \rightarrow \bar{\Lambda}_c\Lambda_c$  and the EMFFs of the  $\Lambda_c$ .— Initial measurements of the  $e^+e^- \rightarrow \bar{\Lambda}_c\Lambda_c$  cross section by the Belle Collaboration [26] indicated the presence of a resonance not too far from the threshold, named  $X(4630)$ , see Fig. 8. Since a resonance with similar mass, the  $Y(4660)$ , had been established in other reactions, like  $e^+e^- \rightarrow \pi^+\pi^-\psi(2S)$  [72], there had been speculations from the very beginning, that one sees the same resonance in the two channels [35, 73]. However, the experiment by the BESIII Collaboration from 2017 [27] signaled a possibly different behavior of the cross section, and the latest measurement by them [28] practically excludes the presence of a resonance. Indeed, now the cross section is more or less constant in the whole threshold region, a behavior quite similar to that observed for  $e^+e^- \rightarrow \bar{\Lambda}\Lambda$  and  $e^+e^- \rightarrow \bar{\Lambda}\Sigma^0 + \text{c.c.}$ . A theoretical interpretation of the new data has been accomplished in [36], based on a  $\bar{\Lambda}_c\Lambda_c$  FSI constructed within chiral effective field theory up to next-to-leading order (NLO). Their results for the cross section are included in Fig. 8, the ones for  $G_E$  and  $G_M$  can be found in [36]. Another interpretation of the data in terms of FSI effects can be found in [42, 43].

Regarding analyses of  $e^+e^- \rightarrow \bar{\Lambda}_c\Lambda_c$  within the VMD approach we want to point to the works by Chen et al. [74, 75] where four charmonium-like states called  $\psi(4500)$ ,  $\psi(4660)$ ,  $\psi(4790)$ , and  $\psi(4900)$  have been included. Earlier studies within the VMD model often focused on the now obsolete  $X(4630)$ . See for example [76].

Interestingly, there is an oscillation in the ratio

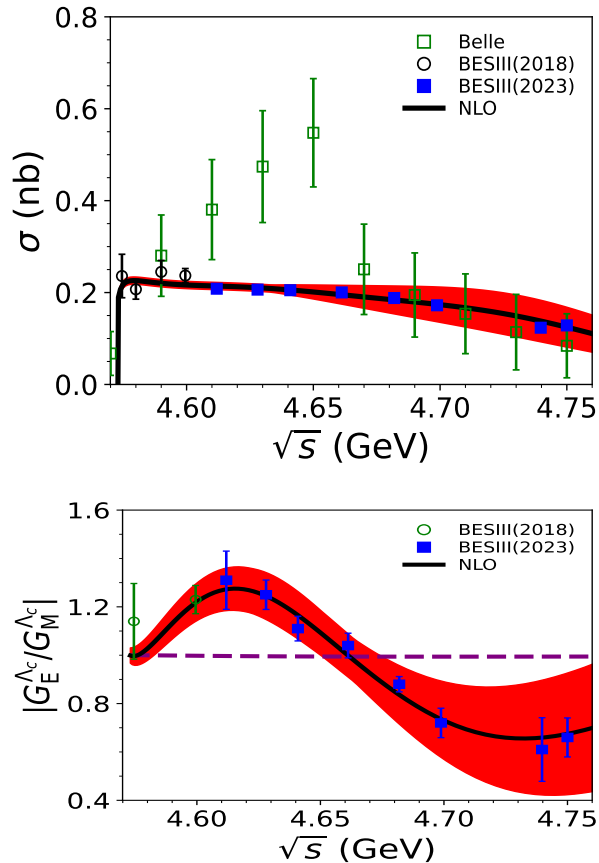


FIG. 8. Cross section for  $e^+e^- \rightarrow \bar{\Lambda}_c\Lambda_c$  and ratio  $|G_E/G_M|$ . Data are from Belle [72] and BESIII [27, 28]. The theory results are by Guo et al. [36] based on an NLO  $\bar{\Lambda}_c\Lambda_c$  FSI.

$|G_E/G_M|$  as measured by BESIII [28]. This feature can be reproduced by considering the  $\bar{\Lambda}_c\Lambda_c$  FSI, see Fig. 8, but also in the VMD approach [74].

*Summary.*— In this Letter, we reviewed the present knowledge of the EMFFs of hyperons in the timelike region. As reported, regarding  $e^+e^- \rightarrow \bar{Y}Y$  cross sections and/or effective form factors, there is already a wealth of data on  $\bar{\Lambda}\Lambda$  and there has been an impressive increase in the database for other hyperon channels over the past few years. In general, theoretical studies can describe the energy dependence of the cross sections (or  $G_{\text{eff}}$ ) reasonably well, in the threshold region by taking into account the  $\bar{Y}Y$  FSI, or over a larger energy range within the conventional VMD model.

On the other hand, for differential observables and/or the individual EMFFs  $G_E$  and  $G_M$  and their relative phase pertinent studies are still in their infancy. For the few channels/energies where data have been published, there is a discrepancy between experiment and theoretical expectations. Moreover, with just few data points available, the energy dependence of the quantities in question cannot be established reliably.

Thus, it is perhaps fair to say that, at present the main unresolved problems and challenges are on the experimental side. For example, there are tensions between some experiments, notably in some  $\bar{\Sigma}\Sigma$  channels. Also, more cross-section data (and with better resolution) are required to firmly establish the energy dependence over the first 100 MeV or so from the thresholds, where effects from the FSI are expected to play an important role. This concerns in particular the  $\bar{\Lambda}\Lambda$  and  $\bar{\Lambda}_c\Lambda_c$  systems with possibly a peculiar near-threshold behavior. And, of course, more differential cross sections and polarization data are needed for a separation of  $G_E$  and  $G_M$  and for determining their relative phase.

Finally, in recent times, there has been a rather strong interest in the apparent oscillations of the  $G_{\text{eff}}$ 's of the proton and neutron in the timelike region [77], see [8] for an extensive list of references. Whether the EMFFs of hyperons exhibit such oscillations too has been addressed in Ref. [78] for the  $\Lambda$ ,  $\Sigma^0$ , and  $\Xi^0$ . It has been found that the present measurements are, in principle, qualitatively compatible with the presence of oscillations. However, due to the large experimental uncertainties in the pertinent data, no firm conclusion can be drawn at present.

*Acknowledgements.*— LYD acknowledges the support from the National Natural Science Foundation of China (NSFC) with Grants No. 12322502, 12335002, Joint Large Scale Scientific Facility Funds of the NSFC and Chinese Academy of Sciences (CAS) under Contract No. U1932110, Hunan Provincial Natural Science Foundation with Grant No. 2024JJ3004, and Fundamental Research Funds for the central universities. The work of UGM was supported by the CAS President's International Fellowship Initiative (PIFI) (Grant No. 2025PD0022) and by the MKW NRW under the funding code No. NW21-024-A and by ERC AdG EX-OTIC (grant No. 101018170).

\* dailingyun@hnu.edu.cn

† j.haidenbauer@fz-juelich.de

‡ meissner@hiskp.uni-bonn.de

- [1] A. Denig and G. Salme, *Prog Part Nucl Phys* **68**, 113 (2013).
- [2] S. Pacetti, R. Baldini Ferroli, and E. Tomasi-Gustafsson, *Phys Rept* **550-551**, 1 (2015).
- [3] L. Xia *et al.*, *Symmetry* **14**, 231 (2022), arXiv:2111.13009 [hep-ex].
- [4] Y.-H. Lin, H.-W. Hammer, and U.-G. Meißner, *Eur Phys J A* **57**, 255 (2021).
- [5] H. Gao and M. Vanderhaeghen, *Rev. Mod. Phys.* **94**, 015002 (2022), arXiv:2105.00571 [hep-ph].
- [6] D. Bisello *et al.* (DM2), *Z Phys C* **48**, 23 (1990).
- [7] B. Aubert *et al.* (BaBar), *Phys. Rev. D* **76**, 092006 (2007), arXiv:0709.1988 [hep-ex].
- [8] Q.-H. Yang, D. Guo, L.-Y. Dai, J. Haidenbauer, X.-W.

- Kang, and U.-G. Meißner, *Sci. Bull.* **68**, 2729 (2023), arXiv:2206.01494 [nucl-th].
- [9] N. H. Buttimore and E. Jennings, *Eur. Phys. J. A* **31**, 9 (2007).
- [10] S. Dobbs *et al.*, *Phys. Lett. B* **739**, 90 (2014), arXiv:1410.8356 [hep-ex].
- [11] M. Ablikim *et al.* (BESIII), *Phys. Rev. D* **97**, 032013 (2018), arXiv:1709.10236 [hep-ex].
- [12] M. Ablikim *et al.* (BESIII), *Phys. Rev. Lett.* **123**, 122003 (2019), arXiv:1903.09421 [hep-ex].
- [13] M. Ablikim *et al.* (BESIII), *Phys. Rev. D* **107**, 072005 (2023), arXiv:2303.07629 [hep-ex].
- [14] M. Ablikim *et al.* (BESIII), *Phys. Rev. D* **109**, 012002 (2024), arXiv:2308.03361 [hep-ex].
- [15] M. Ablikim *et al.* (BESIII), *Phys. Lett. B* **814**, 136110 (2021), arXiv:2009.01404 [hep-ex].
- [16] M. Ablikim *et al.* (BESIII), *Phys. Lett. B* **831**, 137187 (2022), arXiv:2110.04510 [hep-ex].
- [17] M. Ablikim *et al.* (BESIII), *Phys. Rev. Lett.* **132**, 081904 (2024), arXiv:2307.15894 [hep-ex].
- [18] M. Ablikim *et al.* (BESIII), *Phys. Rev. D* **109**, 034029 (2024), arXiv:2312.12719 [hep-ex].
- [19] M. Ablikim *et al.* (BESIII), *JHEP* **05**, 022 (2024), arXiv:2401.09468 [hep-ex].
- [20] G. Gong *et al.* (Belle), *Phys. Rev. D* **107**, 072008 (2023), arXiv:2210.16761 [hep-ex].
- [21] M. Ablikim *et al.* (BESIII), *Phys. Rev. D* **103**, 012005 (2021), arXiv:2010.08320 [hep-ex].
- [22] M. Ablikim *et al.* (BESIII), *Phys. Lett. B* **820**, 136557 (2021), arXiv:2105.14657 [hep-ex].
- [23] M. Ablikim *et al.* (BESIII), *JHEP* **11**, 228 (2023), arXiv:2309.04215 [hep-ex].
- [24] M. Ablikim *et al.* (BESIII), (2024), arXiv:2409.00427 [hep-ex].
- [25] M. Ablikim *et al.* (BESIII), *Phys. Rev. D* **107**, 052003 (2023), arXiv:2212.03693 [hep-ex].
- [26] G. Pakhlova *et al.* (Belle), *Phys. Rev. Lett.* **101**, 172001 (2008), arXiv:0807.4458 [hep-ex].
- [27] M. Ablikim *et al.* (BESIII), *Phys. Rev. Lett.* **120**, 132001 (2018), arXiv:1710.00150 [hep-ex].
- [28] M. Ablikim *et al.* (BESIII), *Phys. Rev. Lett.* **131**, 191901 (2023), arXiv:2307.07316 [hep-ex].
- [29] K. Schönning *et al.*, *Chin. Phys. C* **47**, 052002 (2023), arXiv:2302.13071 [hep-ph].
- [30] J. Haidenbauer, X. W. Kang, and U.-G. Meißner, *Nucl Phys A* **929**, 102 (2014).
- [31] E. Klempt, F. Bradamante, A. Martin, and J. M. Richard, *Phys. Rept.* **368**, 119 (2002).
- [32] X.-W. Kang, J. Haidenbauer, and U.-G. Meißner, *Phys. Rev. D* **91**, 074003 (2015), arXiv:1502.00880 [nucl-th].
- [33] J. Haidenbauer and U.-G. Meißner, *Phys Lett B* **761**, 456 (2016).
- [34] J. Haidenbauer, U.-G. Meißner, and L.-Y. Dai, *Phys Rev D* **103**, 014028 (2021).
- [35] L.-Y. Dai, J. Haidenbauer, and U.-G. Meißner, *Phys Rev D* **96**, 116001 (2017).
- [36] D. Guo, Q.-H. Yang, and L.-Y. Dai, *Phys. Rev. D* **109**, 114005 (2024), arXiv:2404.06191 [hep-ph].
- [37] B. Loiseau and S. Wycech, *Phys. Rev. C* **72**, 011001 (2005), arXiv:hep-ph/0501112.
- [38] D. R. Entem and F. Fernandez, *Phys. Rev. D* **75**, 014004 (2007).
- [39] O. D. Dalkarov, P. A. Khakhulin, and A. Y. Voronin, *Nucl. Phys. A* **833**, 104 (2010), arXiv:0906.0266 [nucl-th].
- [40] G. Y. Chen, H. R. Dong, and J. P. Ma, *Phys. Lett. B* **692**, 136 (2010), arXiv:1004.5174 [hep-ph].
- [41] S. G. Salnikov and A. I. Milstein, *JETP Lett.* **117**, 905 (2023), arXiv:2303.13551 [hep-ph].
- [42] A. I. Milstein and S. G. Salnikov, *Phys. Rev. D* **105**, 074002 (2022), arXiv:2201.07450 [hep-ph].
- [43] S. G. Salnikov and A. I. Milstein, *Phys. Rev. D* **108**, L071505 (2023), arXiv:2309.17018 [hep-ph].
- [44] Z.-S. Jia, Z.-H. Zhang, F.-K. Guo, and G. Li, (2024).
- [45] J. J. Sakurai, *Annals Phys.* **11**, 1 (1960).
- [46] U.-G. Meißner, *Phys. Rept.* **161**, 213 (1988).
- [47] I. T. Lorenz, H. W. Hammer, and U.-G. Meißner, *Phys. Rev. D* **92**, 034018 (2015), arXiv:1506.02282 [hep-ph].
- [48] S. J. Brodsky and G. R. Farrar, *Phys. Rev. D* **11**, 1309 (1975).
- [49] G. P. Lepage and S. J. Brodsky, *Phys Rev Lett* **43**, 545 (1979), [Erratum: *Phys Rev Lett* **43**, 1625–1626 (1979)].
- [50] G. Ramalho, M. T. Peña, and K. Tsushima, *Phys. Rev. D* **101**, 014014 (2020), arXiv:1908.04864 [hep-ph].
- [51] G. Ramalho, *Phys. Rev. D* **103**, 074018 (2021), arXiv:2012.11710 [hep-ph].
- [52] G. Ramalho, M. T. Peña, K. Tsushima, and M.-K. Cheoun, *Phys. Lett. B* **858**, 139060 (2024), arXiv:2407.21397 [hep-ph].
- [53] Y. Yang and Z. Lu, *Mod. Phys. Lett. A* **33**, 1850133 (2018), arXiv:1712.06459 [hep-ph].
- [54] A. Bianconi and E. Tomasi-Gustafsson, *Phys. Rev. C* **105**, 065206 (2022), arXiv:2204.05197 [hep-ph].
- [55] J.-P. Dai, X. Cao, and H. Lenske, *Phys. Lett. B* **846**, 138192 (2023), arXiv:2304.04913 [hep-ph].
- [56] Y.-H. Lin, H.-W. Hammer, and U.-G. Meißner, *Eur. Phys. J. A* **59**, 54 (2023), arXiv:2205.00850 [hep-ph].
- [57] L. Liu and C. S. Fischer, *Eur. Phys. J. A* **60**, 84 (2024), arXiv:2311.13269 [hep-ph].
- [58] B. Kubis and U.-G. Meißner, *Eur. Phys. J. C* **18**, 747 (2001), arXiv:hep-ph/0010283.
- [59] M. Yang and P. Wang, *Phys. Rev. D* **102**, 056024 (2020), arXiv:2005.11971 [hep-ph].
- [60] J. Haidenbauer, T. Hippchen, K. Holinde, B. Holzenkamp, V. Mull, and J. Speth, *Phys. Rev. C* **45**, 931 (1992).
- [61] J. Haidenbauer, K. Holinde, and J. Speth, *Nucl. Phys. A* **562**, 317 (1993).
- [62] X. Cao, J.-P. Dai, and Y.-P. Xie, *Phys. Rev. D* **98**, 094006 (2018).
- [63] Z.-Y. Li, A.-X. Dai, and J.-J. Xie, *Chin. Phys. Lett.* **39**, 011201 (2022), arXiv:2107.10499 [hep-ph].
- [64] Y.-H. Lin, H.-W. Hammer, and U.-G. Meißner, *Eur. Phys. J. C* **82**, 1091 (2022), arXiv:2208.14802 [hep-ph].
- [65] Y. Yang, D.-Y. Chen, and Z. Lu, *Phys. Rev. D* **100**, 073007 (2019), arXiv:1902.01242 [hep-ph].
- [66] L.-Y. Xiao, X.-Z. Weng, X.-H. Zhong, and S.-L. Zhu, *Chin. Phys. C* **43**, 113105 (2019), arXiv:1904.06616 [hep-ph].
- [67] Z.-Y. Bai, Q.-S. Zhou, and X. Liu, *Phys. Rev. D* **108**, 094036 (2023), arXiv:2307.16255 [hep-ph].
- [68] R. Baldini, S. Pacetti, A. Zallo, and A. Zichichi, *Eur. Phys. J. A* **39**, 315 (2009), arXiv:0711.1725 [hep-ph].
- [69] B. Yan, C. Chen, and J.-J. Xie, *Phys. Rev. D* **107**, 076008 (2023), arXiv:2301.00976 [hep-ph].
- [70] Z.-Y. Li and J.-J. Xie, *Commun. Theor. Phys.* **73**, 055201 (2021), arXiv:2012.02379 [hep-ph].
- [71] J. Haidenbauer, K. Holinde, and J. Speth, *Phys. Rev. C* **47**, 2982 (1993).



- [72] X. L. Wang *et al.* (Belle), Phys. Rev. Lett. **99**, 142002 (2007), arXiv:0707.3699 [hep-ex].
- [73] F.-K. Guo, J. Haidenbauer, C. Hanhart, and U.-G. Meißner, Phys. Rev. D **82**, 094008 (2010), arXiv:1005.2055 [hep-ph].
- [74] C. Chen, B. Yan, and J.-J. Xie, Chin. Phys. Lett. **41**, 021302 (2024), arXiv:2312.16753 [hep-ph].
- [75] C. Chen, B. Yan, and J.-J. Xie, (2024), arXiv:2407.19445 [hep-ph].
- [76] J. Wan, Y. Yang, and Z. Lu, Eur. Phys. J. Plus **136**, 949 (2021), arXiv:2102.03092 [hep-ph].
- [77] A. Bianconi and E. Tomasi-Gustafsson, Phys Rev Lett **114**, 232301 (2015).
- [78] A.-X. Dai, Z.-Y. Li, L. Chang, *et al.*, Chin Phys C **46**, 073104 (2022).